

## Interdependence between the magnetic properties and lattice parameters of Ni–Mn–Ga martensite

This article has been downloaded from IOPscience. Please scroll down to see the full text article.

2004 J. Phys.: Condens. Matter 16 8345

(<http://iopscience.iop.org/0953-8984/16/46/020>)

View [the table of contents for this issue](#), or go to the [journal homepage](#) for more

Download details:

IP Address: 129.252.86.83

The article was downloaded on 27/05/2010 at 19:07

Please note that [terms and conditions apply](#).

# Interdependence between the magnetic properties and lattice parameters of Ni–Mn–Ga martensite

V A Chernenko<sup>1</sup>, V A L'vov<sup>2</sup>, V V Khovailo<sup>3</sup>, T Takagi<sup>4</sup>, T Kanomata<sup>5</sup>,  
T Suzuki<sup>5</sup> and R Kainuma<sup>6</sup>

<sup>1</sup> Institute of Magnetism, Kyiv 03142, Ukraine

<sup>2</sup> Radiophysics Department, Taras Shevchenko University, Kyiv 03127, Ukraine

<sup>3</sup> Institute of Radioengineering and Electronics of RAS, Moscow 101999, Russia

<sup>4</sup> Institute of Fluid Science, Tohoku University, Sendai 980-8577, Japan

<sup>5</sup> Department of Applied Physics, Tohoku Gakuin University, Tagajo 985-8537, Japan

<sup>6</sup> Department of Materials Science, Graduate School of Engineering, Tohoku University, Sendai 980-8579, Japan

Received 31 August 2004, in final form 19 October 2004

Published 5 November 2004

Online at [stacks.iop.org/JPhysCM/16/8345](http://stacks.iop.org/JPhysCM/16/8345)

doi:10.1088/0953-8984/16/46/020

## Abstract

The temperature dependences of both the saturation magnetic field values and the powder diffraction patterns of two Ni–Mn–Ga tetragonal martensites were studied experimentally. A reasonable agreement between the temperature dependences of the lattice parameters determined from the x-ray diffraction data and obtained from the magnetization curves is observed. This experimental finding demonstrates the linear dependence of the magnetic anisotropy constant on the tetragonal distortion of the cubic crystal lattice arising in the course of the martensitic transformation, and hence supports the macroscopic and microscopic theories by L'vov *et al* (1998 *J. Phys.: Condens. Matter* **10** 4587) and Enkovaara *et al* (2002 *Phys. Rev. B* **65** 134422), respectively, which predict this dependence.

(Some figures in this article are in colour only in the electronic version)

## 1. Introduction

Recently, a new class of magnetically activated materials (ferromagnetic martensites observed in prototype Ni–Mn–Ga alloys) was widely recognized. In these materials, the ordinary magnetostrictive stresses together with a pliable twinned structure lead to a new set of physical phenomena. Among them, the giant magnetically induced deformation and mechanically driven change of magnetization are of common interest (see [1–9] and references therein).

Ferromagnetic thermoelastic martensites are formed in the  $L2_1$ -ordered Ni–Mn–Ga Heusler alloys as a result of a martensitic transformation (MT). An MT is caused by the Zener-type lattice instability of the initial bcc open crystal structure that forms low-temperature

close-packed tetragonal or orthorhombic structures with different lattice modulations [10, 11]. During this process, uniform shear can be observed with an invariant undistortive habit plane (primary deformation of MT), resulting in the crystallographic correspondence of the martensitic and austenitic lattice [12]. The symmetry properties of austenite and elastic energy minimum conditions imposed on the martensitic phase during its microstructural fragmentation and self-accommodation are the reasons for a considerable degeneracy, manifesting itself in a secondary inhomogeneous lattice invariant deformation by twinning [12].

In accordance with our magnetoelastic model of ferromagnetic martensite [13–16], the interdependence between the magnetic subsystem and aforementioned large deformations in martensitic materials is determined by the spin–lattice magnetoelastic interaction that exists in all solids containing magnetic atoms. This interaction dominates in the formation of a large magnetic anisotropy of the martensitic phase that is proportional to the value of tetragonal distortion of the cubic crystal lattice arising in the course of MT [13–16] (this result of the magnetoelastic model is supported by first-principles calculations [17]). In view of the large value of the uniaxial magnetic anisotropy constant, the secondary deformation (twinning) results in the appropriate spatial distribution of the magnetic moments aligned with the principal axes of the tetragonal unit cells of the martensite variants forming the twin structure. A magnetic field application leads to the rotation of the magnetic moments from the initial crystallographic directions, and therefore the process of magnetization of ferromagnetic martensite provides information about the value of the magnetic anisotropy energy as well as about the volume fractions and orientations of the twin components (martensite variants) [1, 2, 7, 15].

The possible influence of short-period lattice modulations on the magnetic properties of Ni–Mn–Ga martensites was predicted and studied theoretically in [13]. It was shown that the symmetry reduction accompanying the periodic modulation of a tetragonal lattice results in the transformation of the uniaxial magnetic anisotropy energy into a biaxial one, which is characterized by two different anisotropy constants. It should be emphasized that for all structures considered in [13] the value of the saturating magnetic field aligned with  $\langle 100 \rangle$  directions of twin components is proportional to both the magnetoelastic parameter and the value of tetragonal deformation of the cubic crystal lattice characterizing the MT. It is also worth noting that the influence of the symmetry reduction accompanying the short-period lattice modulation on the shape of magnetization curves  $M(H)$  was not observed experimentally, so a uniaxial approximation is commonly used for the theoretical description of the magnetization process in Ni–Mn–Ga martensites and interpretation of the experimental results [2, 3, 16–18]. In particular, the magnetic anisotropy energy of the different Ni–Mn–Ga martensites was studied as a function of temperature, suggesting its single ion origin [18].

It was mentioned above that both the phenomenological magnetoelastic model [13–16] and *ab initio* calculations [17] predict a linear dependence of the magnetic anisotropy parameter of Ni–Mn–Ga martensite on the spontaneous strains  $\varepsilon_{ii}$  which are proportional to the tetragonal distortion of a cubic crystal lattice occurring in the course of an MT ( $\varepsilon_{ii} \sim (c - a)/a_0$ , where  $a$  and  $c$  are the lattice parameters of the tetragonal phase, and  $a_0$  is the lattice parameter of the cubic phase). In the present work, this fundamental theoretical result is confirmed experimentally by the comparison of the temperature dependence of lattice parameters determined from the x-ray diffraction data with the dependence resulting from the theoretical treatment of magnetization curves taken for two different Ni–Mn–Ga ferromagnetic martensites. The research proceeds as follows: measurements of the saturation magnetic field as a function of temperature  $H_s(T)$  are carried out; these measurements allow us to determine the  $c/a(T)$  dependence according to phenomenological theory; then, the latter dependence is compared with the  $c/a(T)$  function obtained by the x-ray diffraction method.

## 2. Theoretical background

The theoretical value of the saturation magnetic field  $H_s$  results from the expression for the non-isotropic part  $F$  of the magnetic energy. For the ferromagnetic tetragonal martensitic phase exposed to an external magnetic field, this energy is expressed as

$$F = Am_x^2 + \frac{M^2(\mathbf{m} \cdot \mathbf{D} \cdot \mathbf{m})}{2} - \mathbf{mHM} \quad (1)$$

where the first term describes the magnetic anisotropy energy of a crystal lattice with the  $c$ -axis oriented in the  $x$ -direction. The second and third terms present the magnetostatic and Zeeman energies, respectively.  $M$  denotes the absolute value of the magnetization,  $\mathbf{D}$  is a demagnetization matrix, and  $\mathbf{m} = \mathbf{M}/M$ . The phenomenological model of ferromagnetic martensite [13] relates the magnetoelastic parameter  $\delta_1$  that characterizes a cubic parent phase to the magnetic anisotropy constant  $A$  and the lattice parameters  $a$ ,  $c$  of the tetragonal phase. This relationship corresponds to a linear approximation of the small lattice distortion  $1 - c/a$ . It is convenient to present this relationship in the form of  $A = 6\delta_1(1 - c/a)$  (see [15, 16]). When  $\delta_1 < 0$  the vector  $\mathbf{m}$  of Ni–Mn–Ga martensite with  $c/a < 1$  is parallel to the  $c$ -axis in zero magnetic field.

Let the specimen be a rotation ellipsoid with the rotation axis located in the  $y$ -direction. In such a case,  $\mathbf{D}$  is a diagonal matrix with the elements  $D_1 = D_3 \neq D_2$ . The standard minimization procedure for the energy in equation (1) shows that the magnetic field applied in the  $y$ -direction causes a rotation of the vector  $\mathbf{m}$  in the  $xy$  plane at an angle of  $\psi = \arccos(H/H_s)$ , and hence magnetic saturation occurs when

$$H = H_s = M[D_2 - D_1 + 12|\delta|(1 - c/a)], \quad (2)$$

where the dimensionless magnetoelastic parameter  $\delta$  is defined as  $\delta = \delta_1/M^2$ . Equation (2) results in the following expression for the lattice tetragonality in the martensitic phase:

$$c/a = 1 - \frac{[(H_s/M) + |D_1 - D_2|]}{12|\delta|}. \quad (3)$$

Equations (2) and (3) establish the interrelation between  $H_s$  and the  $c/a$  ratio. Accordingly, the dependence of the  $c/a$  ratio on the different thermodynamic factors (e.g. temperature or alloy composition) should correlate with the behaviour of  $H_s$ . In particular, a linear dependence between the  $H_s/M$  and  $c/a$  ratios must be observed since the dimensionless magnetoelastic parameter weakly depends on the temperature [19] (the values of the elements of the demagnetization matrix are prescribed by the specimen shape). The structural analysis shows that the tetragonality of the Ni–Mn–Ga martensites strongly depends on the temperature [20–22]. According to equation (3), the temperature dependence of the  $c/a$  ratio can also be derived from the values of the magnetic saturation field measured for the different temperatures. More accurate treatment of the results during this procedure implies that the temperature change of the magnetization values  $M$  corresponding to the nearly horizontal segments of magnetization curves at different temperatures is taken into account (see section 4).

## 3. Experimental details

Two alloys in both single-crystalline and polycrystalline forms with compositions  $\text{Ni}_{49.5}\text{Mn}_{25.4}\text{Ga}_{25.1}$  (denoted as A1) and  $\text{Ni}_{52.6}\text{Mn}_{23.6}\text{Ga}_{23.8}$  (A2) exhibiting low-temperature and ambient-temperature martensitic transformations, respectively, were studied. The characteristic temperatures  $T_M = 170$  K,  $T_A = 180$  K,  $T_C = 381$  K for A1 and  $T_M = 284$  K,  $T_A = 297$  K,  $T_C = 363$  K for A2 ( $T_M$  and  $T_A$  are the forward and reverse martensitic

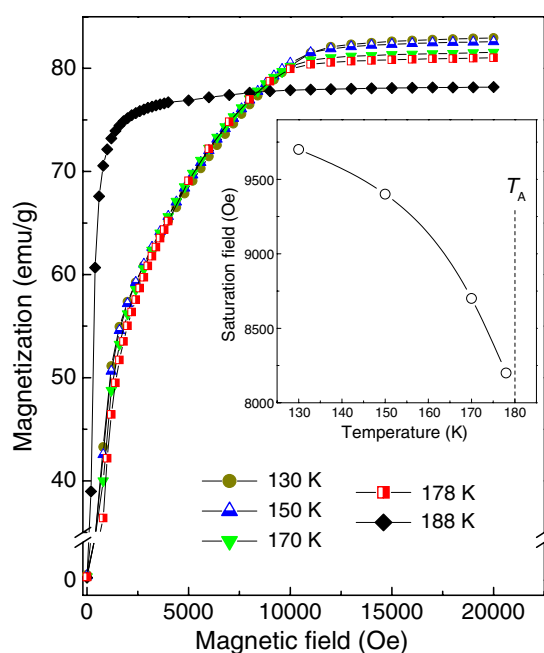


**Figure 1.**  $M(H)$  curves measured along the  $(100)_p$  axis of an A1 single crystal at different constant temperatures during heating in the martensitic state:  $T = 130$ – $178$  K and at  $T = 188$  K corresponding to austenite. Inset: the change of saturation field as a function of temperature. The curved line is a guide for the eyes. The position of the temperature  $T_A$  is indicated by the dashed line.

transformation temperatures and  $T_C$  is the Curie temperature) were obtained as the points corresponding to the half anomalies on the temperature dependences of the low-field magnetic susceptibility. Single-crystalline parallelepiped-shaped samples of  $3.5 \times 0.75 \times 0.75$  mm<sup>3</sup> for A1 and  $7.0 \times 1.0 \times 1.0$  mm<sup>3</sup> for A2 with their long axes oriented in the  $\langle 100 \rangle$  direction were prepared for the magnetization measurements. The magnetization curves  $M(H)$  were measured at constant temperatures using a superconducting quantum interference device (Quantum Design MPMS SQUID magnetometer). In these measurements, the magnetic field was oriented along the long axis of the samples.

A disc cut from a polycrystalline ingot of an alloy with composition and transformation temperatures being similar to A1 and vacuum-annealed at 1073 K for 2 h as well as powder of alloy A2, prepared by mortar-and-pestle grinding of the single-crystal and vacuum-annealed at 873 K for 10 h were used for the x-ray measurements. The x-ray diffraction (XRD) patterns at various constant temperatures were obtained by the powder method using a Rigaku RINT2000 x-ray diffractometer (Cu  $K\alpha$  radiation).

#### 4. Results and discussion

Application of the magnetic field to the martensitic alloy initiates the following processes: (i) reversible displacements of  $180^\circ$  magnetic domain walls, (ii) reversible rotation of the magnetic vectors in twin variants, and (iii) irreversible reorientation of twin variants. The negligible difference between the experimental field-increase and field-decrease magnetization curves obtained in the present work allows us to disregard process (iii) in our samples and to present only field-increase results in figures 1 and 2. One of the  $M(H)$  curves shown in figure 1

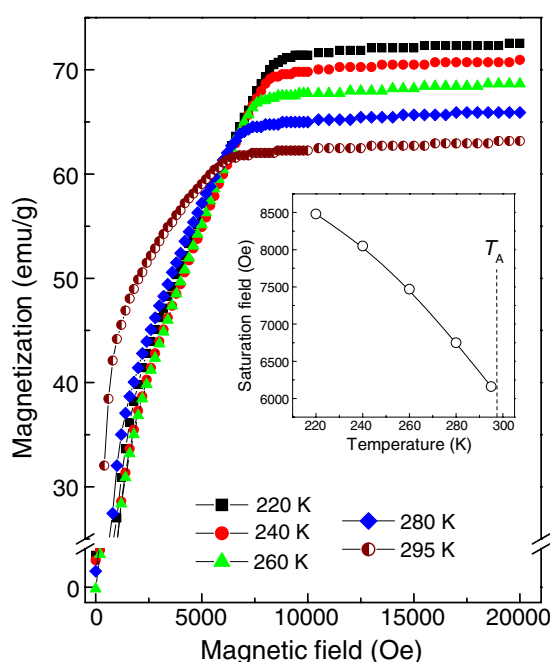


**Figure 2.**  $M(H)$  curves measured along the  $\langle 100 \rangle_p$  axis of an A2 single crystal at different constant temperatures during heating in the martensitic state:  $T = 220$ – $295$  K. Inset: saturation field as a function of temperature. The curved line is a guide for the eyes. The position of the temperature  $T_A$  is indicated by the dashed line.

was measured in the austenitic state of the samples. For the austenitic phase, the saturating field value corresponds to the end of process (i) (see figure 1, curve at 188 K) because of the very low magnetic anisotropy energy of the cubic crystal lattice. The other magnetization curves presented in figures 1 and 2 are taken in martensitic state (a mixed austenitic–martensitic state can take place at 295 K (figure 2)). It can be deduced from the shapes of these curves that the specimens contain a mixture of twin components. The twins with a  $c$ -axis oriented along the long edges of both samples contribute to the magnetization process (i) while the remaining part of each sample containing twins with a transversal orientation of  $c$ -axes contributes mainly to the magnetization process (ii), thereby providing the possibility of a determination of the  $c/a$  ratio from the  $H_s$  values observed. The numerical values of the saturating magnetic field have been determined from the slopes of  $M(H)$  curves by a tangential method, i.e., as the coordinates of the cross points of the linearly extrapolated slope of the magnetization line in the high-field region and its slope in the field interval corresponding to process (ii). Such a procedure results in an uncertainty of about 100 Oe for the absolute values of  $H_s$  for alloy A2 (figure 2). The choice of the start and end point of the tangent in a range of the increasing slope of magnetization in figure 1 seems to be arbitrary. Nevertheless, consistent results of the relative change of  $H_s$  can be extracted. If data points of magnetization in the same reduced magnetic field intervals are used to construct the tangents, the total change of  $H_s$  in the temperature range studied is obtained to be equal to about 1500 Oe in each field interval. In this case, the uncertainty in relative values of  $H_s$  is less than 200 Oe. The absolute values of  $H_s$  can be also read as the points where the curved parts of the  $M(H)$  graphs touch the straight lines drawn across the experimental points at the high fields. Within the error bars both methods described above provide a similar relative change of  $H_s$ . The nonlinear evolutions of  $H_s$  are shown in the

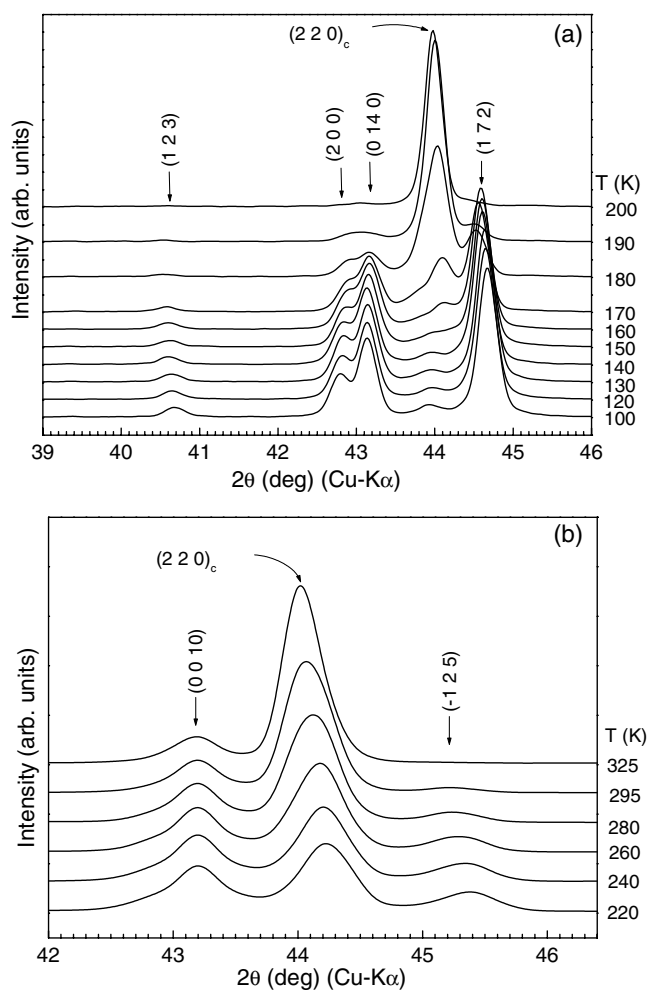


**Figure 3.** Temperature evolution of the main XRD reflections of A1 (a) and A2 (b) samples measured at constant temperatures during heating. The indexing refers to the monoclinic system.

insets of figures 1 and 2. The nearly horizontal segments of the magnetization curves provide the magnetization values  $M$ , which are involved in the equation (3).

The temperature dependences of the fragments of the XRD patterns for both alloys are shown in figure 3. The indexing is made in the monoclinic system [11, 23]. The peaks obtained for the austenitic cubic phase are also indicated.

The whole diffraction pattern for the martensitic phase in alloy A1 is accounted for by the seven-layered modulated orthorhombic unit cell and space group  $Pn\bar{1}m$  described in [24]. The lattice parameters of this unit cell are  $a_{\text{ortho}} = 0.4225$  nm,  $b_{\text{ortho}} = 2.9331$  nm and  $c_{\text{ortho}} = 0.5532$  nm at  $T = 100$  K. It can be seen that the value of orthorhombic distortion is about 1%. Hence it may be disregarded hereafter. Translation of the above lattice parameters into cubic coordinate axes provides a tetragonal unit cell with lattice parameters  $a = 0.5973$  nm and  $c = 0.5532$  nm [11]. The tetragonal lattice parameters of alloy A1 have been obtained at each temperature, and their ratios are plotted in figure 4(a). They show a roughly linear dependence which agrees with the results of [21].

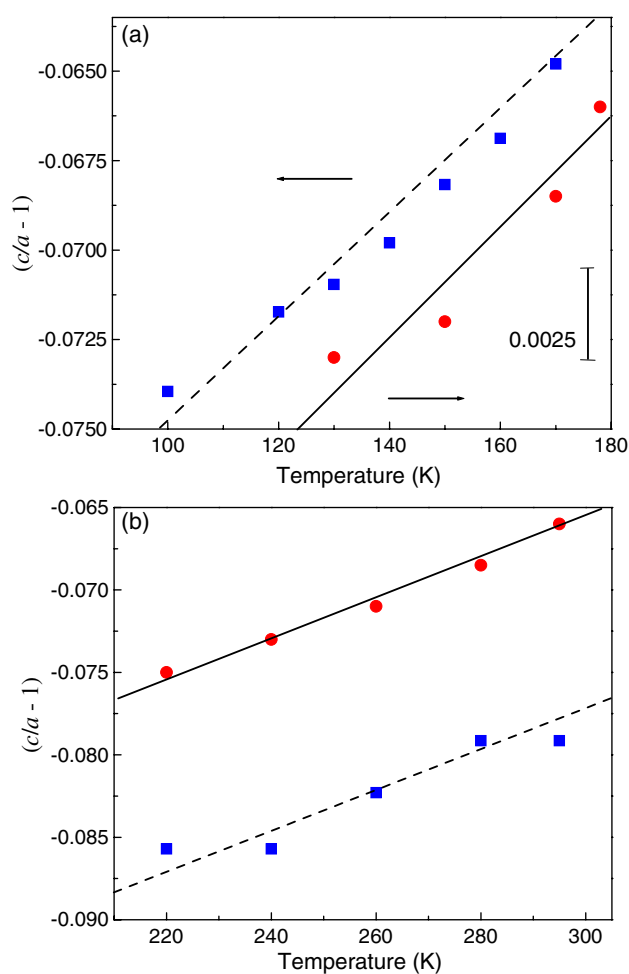


**Figure 4.** Temperature dependence of the lattice distortion accompanying the cubic–tetragonal martensitic transformations in alloys A1 (a) and A2 (b) as determined from x-ray measurements (squares) and computed from equation (3) using magnetization measurements (circles). The symbol size corresponds to the error bar. The lines are linear fits.

For the powdered alloy A2, a similar analysis of x-ray results was hindered due to reduced intensities of peaks and traces of another phase(s) (presumably MnO) in the diffraction pattern. Nevertheless, we found that the austenitic reflection (220) in figure 3(b) is split into two and that this pair of most intensive reflections can be assigned to the tetragonal unit cell. Then, the  $c/a$  ratio was calculated directly at different temperatures. Thus, accumulation of errors related to the absolute determination of the lattice parameters is avoided. The results are shown in figure 4(b). We studied recently the alloy A2 in a single-crystalline form by *in situ* transmission electron microscopy and found a five-layered tetragonal martensitic structure [25]. Since both x-ray diffraction and electron microscopy provide a tetragonal unit cell for the martensite, the results for the powdered alloy A2 (figure 3(b)) were adequate to compare with the magnetization measurements made on the same alloy in a bulk form.

In figure 4, the structural results obtained from x-ray measurements are compared with those calculated from equation (3) using experimentally obtained saturation fields and



magnetization values read at different temperatures. The previously reported values of  $\delta = -23$  (see [15, 16]) and  $\rho = 8 \text{ g cm}^{-3}$  ( $\rho$  is the mass density) were used for the calculations. The temperature dependences of the lattice distortion for both alloys can be approximated by a linear dependence.

The most striking and important result is that the slopes of the lines reflecting the structural and magnetic features for each alloy can be treated in the first approximation as identical<sup>7</sup>. This strongly supports the validity of equation (3) derived from the magnetoelastic model of ferromagnetic martensite. This model shows that the large magnetic anisotropy parameter of the ferromagnetic martensite is strictly proportional to the value of spontaneous shear strain caused by the MT in the ferromagnetic austenitic phase, where sufficiently strong magnetoelastic interaction exists. The results obtained also confirm that the dimensionless magnetoelastic parameter weakly depends on the temperature.

### Acknowledgment

VAC is grateful to the Japan Society for the Promotion of Science for Fellowship grant ID No. RC30326005.

### References

- [1] Ullakko K, Huang J K, Kantner C, O'Handley R C and Kokorin V V 1996 *Appl. Phys. Lett.* **69** 1966
- [2] O'Handley R C 1998 *J. Appl. Phys.* **83** 3263
- [3] James R D and Wuttig M 1998 *Phil. Mag. A* **77** 1273
- [4] O'Handley R C, Murray S J, Marioni M, Nembach H and Allen M S 2000 *J. Appl. Phys.* **87** 4712
- [5] Likhachev A, Sozinov A and Ullakko K 2003 *J. Physique IV* **112** 981
- [6] Müllner P, Chernenko V A and Kostorz G 2003 *Scr. Mater.* **49** 129
- [7] Pasquale M, Sasso C P, Bertotti G, L'vov V A, Chernenko V A and De Simone A 2003 *J. Appl. Phys.* **93** 8641
- [8] Vasil'ev A N, Buchel'nikov V D, Takagi T, Khovailo V V and Estrin E I 2003 *Phys.—Usp.* **46** 559
- [9] Chernenko V A, L'vov V A, Müllner P, Kostorz G and Takagi T 2004 *Phys. Rev. B* **69** 134410
- [10] Webster P J, Ziebeck K R A, Town S L and Peak M S 1984 *Phil. Mag. B* **49** 295
- [11] Pons J, Chernenko V A, Santamarta R and Cesari E 2000 *Acta Mater.* **48** 3027
- [12] Lieberman D S, Read T A and Wechsler M S 1957 *J. Appl. Phys.* **28** 532
- [13] L'vov V A, Gomonaj E V and Chernenko V A 1998 *J. Phys.: Condens. Matter* **10** 4587
- [14] Chernenko V A, L'vov V A and Cesari E 1999 *J. Magn. Magn. Mater.* **196/197** 859
- [15] L'vov V, Zagorodnyuk S, Chernenko V and Takagi T 2002 *Mater. Trans.* **43** 876
- [16] Chernenko V A, L'vov V A, Zagorodnyuk S P and Takagi T 2003 *Phys. Rev. B* **67** 064407
- [17] Enkovaara J, Ayuela A, Nordström L and Nieminen R M 2002 *Phys. Rev. B* **65** 134422
- [18] Straka L and Heczko O 2003 *J. Appl. Phys.* **93** 8636
- [19] Chernenko V A, L'vov V A, Pasquale M, Sasso C P, Besseghini S and Polenur D A 2000 *Int. J. Appl. Electromagn. Mech.* **12** 1
- [20] Ma Y, Awaji S, Watanabe K, Matsumoto M and Kobayashi N 2000 *Solid State Commun.* **113** 671
- [21] Okamoto N, Nakamura Y, Fukuda T, Kakeshita T, Takeuchi T and Kishio K 2003 *Trans. Mater. Res. Soc. Japan* **28** 245
- [22] Glavatska N, Mogilniy G, Glavatsky I, Danilkin S, Hohlwein D, Beskrovniy A, Soderberg O and Lindroos V K 2003 *J. Physique IV* **112** 963
- [23] Ge Y, Soderberg O, Lanska N, Sozinov A, Ullakko K and Lindroos V K 2003 *J. Physique IV* **112** 921
- [24] Brown P J, Crangle J, Kanomata T, Matsumoto M, Neumann K-U, Ouladiaz B and Ziebeck K R A 2002 *J. Phys.: Condens. Matter* **14** 10159
- [25] Segui C, Chernenko V A, Pons J, Cesari E, Khovailo V and Takagi T 2004 *Acta Mater.* at press

<sup>7</sup> The absolute value of the shift between the lines presented in figure 4 is less than 10% and can be attributed to the uncertainty range of the  $\delta$  value.